Emergence of new quasiparticles in quantum electrodynamics at finite temperature

Gordon Baym
Department of Physics, University of Illinois at Urbana-Champaign, 1110 West Green Street, Urbana, Illinois 61801

Jean-Paul Blaizot
Service de Physique Théorique, Centre d'Etudes Nucléaires, Saclay, 91191 Gif-sur-Yvette, France

Benjamin Svetitsky
School of Physics and Astronomy, Raymond and Beverly Sackler Faculty of Exact Sciences, Tel Aviv University, 69978 Tel Aviv, Israel

(Received 22 May 1992)

We study the spectrum of fermionic excitations in a hot relativistic electron plasma. Numerical analysis of the one-loop electron propagator shows the appearance of new quasiparticle modes, as already studied in the massless fermion limit, as the temperature is raised to exceed the electron mass m. We calculate the relevant spectral densities and show that one mode, whose splitting in energy from the original electron is of the order of m, moves as the temperature is raised towards higher frequency along with the electron while retaining a narrow width. We compare results derived in Feynman and Coulomb gauges. The role of the zero-temperature counterterms is discussed.

PACS number(s): 12.20.Ds, 52.55.Mg, 52.60.+h

I. INTRODUCTION

In studies of the elementary fermion excitations of a hot relativistic quark-gluon plasma, it was found that the spectrum develops a gap of order gT at zero momentum, where g is the coupling constant and T the temperature, and that at finite momentum the spectrum is split [1–6]. In this paper we study this phenomenon in the Yukawa theory (electrons interacting by exchange of massless scalar "photons") and in QED, focusing particularly on how the spectrum changes as the temperature is raised. We find that a number of new poles appear in the fermion propagator at various threshold temperatures, of which only one corresponds to a state narrow enough to be considered a quasiparticle. As we shall see, the new modes in the spectrum do not appear in a discrete transition; rather broad spectral weight in the neighborhood of the new excitations sharpens with increasing temperature.

Previous authors (with the exception of Refs. [5–7]) have concentrated on the physics of massless fermions or, in other words, on the extreme relativistic limit in which $T \gg m$, where m is the bare fermion mass. Figure 1 shows the fermion dispersion relation found to second order in the coupling, when the mass is neglected. (We consider only the case of zero chemical potential. A discussion of what happens with a finite chemical potential will be given in [9]). In order to see how this spectrum comes about as the temperature is raised from zero, we confine our attention below to the situation at zero quasiparticle momentum, $\mathbf{p}=0$. Just as a small nonzero $\mathbf{p}$ splits the dispersion relation, a nonzero mass splits the state at $\mathbf{p}=0$. Moreover, just as a *large* $\mathbf{p}$ broadens the new (lower) state and makes it disappear from the spectrum [5], a sufficiently large mass does the same. In fact the new state has features of a collective excitation, and as such its presence in the spectrum is expected only when p and $m \lesssim gT$. Turning this argument around: for fixed m at $\mathbf{p}=0$, one expects that a new fermion state, split from the original fermion, will gather strength as T is raised past m/g and become, as T increases, a quasiparticle, eventually as narrow as the (now-broadened) original fermion. This new quasiparticle has been dubbed the "plasmino" by Braaten and Pisarski [8].

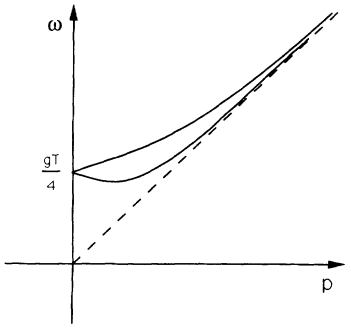

FIG. 1. Spectrum of electron excitations in an ultrarelativistic plasma. The upper branch is the "normal" electron state. The dashed line is the line $\omega=p$.

In the next section we study the Yukawa theory, introducing the many-body formalism we employ. We display explicitly the poles of the propagator and the corresponding peaks in the spectral densities. We use throughout $g^2/4\pi \equiv \alpha = 1/137$ so that $1/g \simeq 3.3$. In Sec. III we apply the same analysis to QED. Our main result is that a new electron state appears gradually at $T \simeq 3m$. At that point the electron has shifted to $\omega \simeq 1.1m$, and the new peak in the spectral density is at $\omega \simeq 0.1m$. As the temperature is raised further, both peaks move off together towards higher ω, maintaining the splitting of order m as their shapes change.

Since our analysis in the case of QED is based on the

electron propagator which is a gauge-dependent object, the question of gauge invariance arises. As is well known, irrespective of the temperature, the location of well-defined poles in the propagator is gauge independent, since the poles correspond to physical excitations. (For a recent discussion, see [10,11].) The full spectral weight is not necessarily gauge independent; moreover, one-loop calculations are insufficient to account correctly for the widths of the quasiparticles. Since our calculation is limited to one loop, we expect our results for intermediate values of the temperature to be gauge dependent, and this is indeed what we find by comparing, for the sake of illustration, calculations in Feynman and Coulomb gauges. As it turns out, the peak positions appear to coincide in the two gauges for the entire temperature range studied, while the widths are different. To go systematically beyond leading order requires resummation of higher-order loops [8,12].

We discuss in Sec. IV the oft-neglected zero-temperature piece of the propagator. It has usually been tacitly assumed that its effects vanish into renormalization counterterms. In fact, the finite-temperature shift of the electron off its mass shell makes it necessary to take into account an infrared-divergent zero-temperature contribution to the inverse propagator, which gives a further shift in the dispersion relation. This also applies to the new quasiparticle, which of course is not on the original electron mass shell, either. We include this contribution with the aid of an infrared cutoff, and show that our results are essentially unchanged for reasonable values of the cutoff. Removal of this cutoff will have to await a more systematic analysis.

II. YUKAWA THEORY

Consider the coupling of a Dirac fermion ψ to a massless scalar field ϕ with the interaction $q\phi\bar{\psi}\psi$. Because this case shares the basic features of the fermionic spectrum of QED, which we discuss in the next section, we shall refer to the fermion as an "electron" and to the scalar particle as a "photon." The electron modes are given by the poles of the Green's function $G(\mathbf{p},\omega)$, where

$$G^{-1}(\mathbf{p},\omega)=G_0^{-1}(\mathbf{p},\omega)-\Sigma(\mathbf{p},\omega)\ . \tag{1}$$

The free particle propagator is

$$G_0^{-1}(\mathbf{p},\omega)=\omega\gamma_0-\gamma\cdot\mathbf{p}-m\ , \tag{2}$$

and the self-energy Σ has the structure

$$\Sigma(\mathbf{p},\omega)=a\gamma_0+b\gamma\cdot\mathbf{p}+c\ , \tag{3}$$

where a,b, and c are functions of ω and $|\mathbf{p}|$, and thus

$$G^{-1}(\mathbf{p},\omega)=(\omega-a)\gamma_0-(1+b)\gamma\cdot\mathbf{p}-(c+m)\ . \tag{4}$$

The temperature-dependent part of the one-loop self-energy, illustrated in Fig. 2, is given in the limit $\mathbf{p}=0$ by

$$\Sigma(0,\omega)=g^2\int\frac{d^3k}{(2\pi)^3 2k}\left[\frac{\epsilon_k\gamma_0+m}{2\epsilon_k}\left[\frac{n_k-f_k}{\omega-\epsilon_k-k}+\frac{n_k+f_k}{\omega-\epsilon_k+k}\right]+\frac{\epsilon_k\gamma_0-m}{2\epsilon_k}\left[\frac{n_k-f_k}{\omega+\epsilon_k+k}+\frac{n_k+f_k}{\omega+\epsilon_k-k}\right]\right], \tag{5}$$

where $\epsilon_p=\sqrt{p^2+m^2}$ and $k=|\mathbf{k}|$. The thermal factors are

$$f_p=\frac{1}{e^{\beta\epsilon_p}+1}\ ,\quad n_k=\frac{1}{e^{\beta k}-1}\ , \tag{6}$$

where $\beta=1/T$. The self-energy has the form $\Sigma(0,\omega)=a(\omega)\gamma_0+c(\omega)$. The four terms in Eq. (5) correspond to the processes shown in Fig. 3.

In the high-temperature limit, $T\gg m$, one can ignore $c\propto m$ in Σ. The main contributions to the integral in Σ come from the region $k\simeq T$. The leading terms in a correspond to two processes: one in which a scalar photon with momentum k is absorbed, producing an electron with momentum k [Fig. 3(c)], and one in which a positron with momentum k annihilates with the initial electron into a photon with momentum k [Fig. 3(b)]. For both these processes the energy of the particle in the thermal bath cancels that of the intermediate state, and

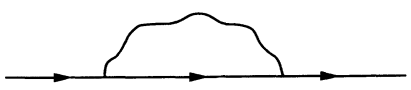

FIG. 2. Electron self-energy to order one loop.

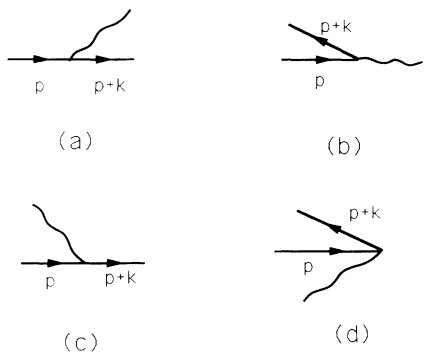

FIG. 3. Physical processes contributing to the imaginary part of the fermion self-energy. Processes (b) and (c) are the dominant ones at high temperature.

the denominators in Eq. (5) reduce to that of the incident particle, namely ω. Then a is simply given by

$$a(\omega)=\frac{g^2}{\omega}\int\frac{d^3k}{(2\pi)^3 2k}(n_k+f_k)=\frac{g^2T^2}{16\omega}\ . \tag{7}$$

The poles of

$$G(0,\omega)=\frac{\gamma_0}{\omega-g^2T^2/16\omega} \tag{8}$$

are then at $\omega=\pm gT/4$.

The energies of the states look like those of free fermions with mass $gT/4$. However, the interactions in the heat bath produce a mixing between the positive- and negative-energy solutions of the free Dirac equation which results in a richer structure than that of a free particle spectrum. To a certain extent, this structure is dictated by symmetry considerations. The single particle Hamiltonian, $H=\omega-\gamma_0 G^{-1}$, at $\mathbf{p}=0$ commutes with both γ_5 and γ_0. Since γ_5 and γ_0 do not commute, eigenstates of H (or of G) must be degenerate. For massless free particles this degeneracy is realized by the positive and negative energy branches for nonzero $\mathbf{p}$ meeting at $\omega=0$ when $\mathbf{p}\to 0$. Here, however, the existence of the gap $gT/4$ forces an additional degeneracy on the system. Consider, for example, a state with $\omega=gT/4$ and $\gamma_0=+1$. Acting on it with γ_5 flips it to a state with $\gamma_0=-1$, leaving its energy unchanged. There are thus four degenerate states at energy $gT/4$ and four at energy $-gT/4$, and each group of states exhausts the possible quantum numbers which may be attributed to a Dirac spinor. Two of the states with $\omega=gT/4$ have helicity equal to their chirality, and two have helicity opposed to chirality. [This is easily seen by multiplying Eq. (4) by $\gamma_5\gamma_0$.] For fuller discussion of the symmetry properties of the massless spectrum, see [13,4]. The degeneracy at $\mathbf{p}=0$ is broken at nonzero p, giving the two branches seen in Fig. 1. A similar splitting appears at $p=0$ when the fermion mass m is nonzero.

At zero temperature, the spectrum ϵ_p is that of free fermions of mass m; at low temperatures the spectrum undergoes a small shift through the coupling to the thermal bath of photons. How then does the richer structure seen in Fig. 1 develop as the temperature is raised? To answer this question we study the poles and the spectral weight of the Green's function $G(0,\omega)$ as the temperature is raised. It is useful to decompose G according to the eigenvalues of γ_0. From Eqs. (1)–(3), it follows that at an arbitrary temperature

$$G(\omega)=\left[\frac{1+\gamma_0}{2}\right]G_+(\omega)-\left[\frac{1-\gamma_0}{2}\right]G_-(\omega)\ , \tag{9}$$

where

$$G_\pm(\omega)=\frac{1}{\omega\mp m-(a\pm c)}\ . \tag{10}$$

The Green's functions $G_\pm$ can be written in terms of their spectral densities $\mathcal{A}_\pm$ as

$$G_\pm(\omega)=\int\frac{d\omega'}{2\pi}\frac{\mathcal{A}_\pm(\omega')}{\omega-\omega'}\ . \tag{11}$$

Since $G_-(\omega)=-G_+(-\omega)$, the spectral functions are related according to $\mathcal{A}_-(-\omega)=-\mathcal{A}_+(\omega)$.

First we trace the roots of the real part of the denominators $\omega\mp m-(a\pm c)$ in G. Wherever the imaginary part of the self-energy, which we examine below, is small, these roots correspond to well-defined quasiparticle modes. Since c is even in ω, and a odd, the solutions of $\omega+m-\mathrm{Re}(a-c)=0$, corresponding to $\gamma_0=-1$, are just the negatives of the solutions of $\omega-m-\mathrm{Re}(a+c)=0$, corresponding to $\gamma_0=1$. Explicitly,

$$\mathrm{Re}(a\pm c)=g^2P\int\frac{d^3k}{(2\pi)^3 4k}\left[\left[1\pm\frac{m}{\epsilon_k}\right]\left[\frac{n_k-f_k}{\omega-\epsilon_k-k}+\frac{n_k+f_k}{\omega-\epsilon_k+k}\right]+\left[1\mp\frac{m}{\epsilon_k}\right]\left[\frac{n_k-f_k}{\omega+\epsilon_k+k}+\frac{n_k+f_k}{\omega+\epsilon_k-k}\right]\right], \tag{12}$$

where P denotes a principal value.

The shapes of the functions $\mathrm{Re}(a\pm c)$ for positive ω are shown in Fig. 4. At $\omega=0$,

$$c(0)=-\frac{g^2}{m}\int\frac{d^3k}{(2\pi)^3}\left[\frac{n_k}{k}+\frac{f_k}{\epsilon_k}\right]<0\ , \tag{13}$$

while $a(0)=0$. Similarly,

$$\left.\frac{\partial a}{\partial\omega}\right|_{\omega=0}=-\frac{g^2}{m^4}\int\frac{d^3k}{(2\pi)^3 k}[n_k(2k^2+m^2)+2k\epsilon_k f_k]<0\ , \tag{14}$$

while $(\partial c/\partial\omega)_{\omega=0}=0$. Thus at small T/m, the equation $\mathrm{Re}(a+c)=\omega-m$ has one root, $\omega\simeq m$, corresponding to the free particle solution. As the temperature increases, $c(0)$ becomes more and more negative, and the negative slope at the origin increases in magnitude, so that eventually the curve of $\mathrm{Re}(a+c)$ begins to intersect the line $\omega-m$ in two more places, at small ω/m [Fig. 4(a)]. For larger temperatures, $c(0)$ becomes more negative than $-m$, and the lower root moves to negative ω [Fig. 4(b)]. The behavior of the $\gamma_0=-1$ branch is seen in Fig. 4(c). For small T/m, the value of $\mathrm{Re}(a-c)$ is always smaller than $\omega+m$, so that there are no positive roots. However,

with increasing T, as seen in Fig. 4(c), the curve of $\mathrm{Re}(a-c)$ intersects the line $\omega+m$ twice. The upper of these two roots becomes the $\gamma_0=-1$ partner of the $\gamma_0=+1$ quasiparticle state. The lower root with $\gamma_0=-1$ stays at small ω when the temperature rises. When the y intercept of the curve, which is equal to $-c(0)$, exceeds m, another $\gamma_0=-1$ root moves from negative to positive ω. For large temperatures, these roots accumulate in a narrow interval above $\omega=0$. The flow of the roots for all ω and $\gamma_0=\pm1$ is shown in Fig. 5.

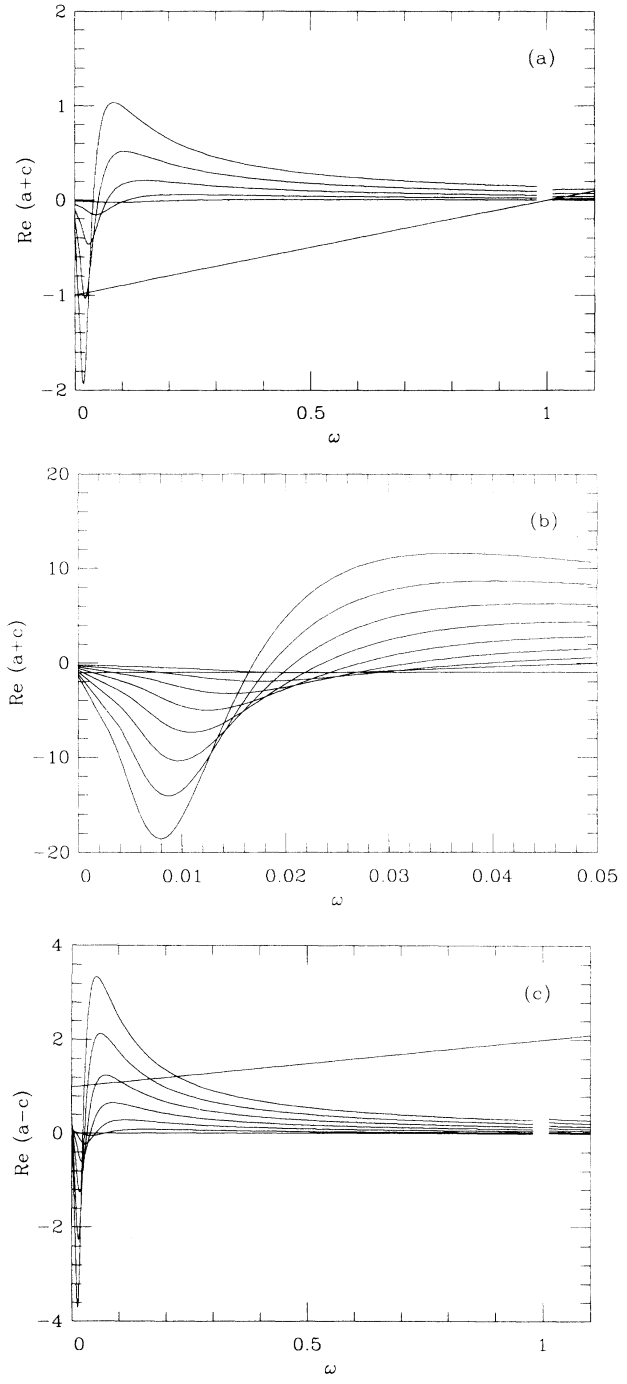

FIG. 4. (a) $\mathrm{Re}[a(\omega)+c(\omega)]$ for $T=1,2,3,4,5$ (in order of increasing amplitude). We have set $m=1$ and $g^2/4\pi=1/137$ in this and all following figures. The area around $\omega=1$ is omitted because of numerical difficulties. The straight line is $(\omega-m)$. (b) Same, for $T=4,5,\ldots 11$, emphasizing structure at small ω. The straight line is again $(\omega-m)$. (c) $\mathrm{Re}[a(\omega)-c(\omega)]$ for $T=1,2,\ldots 7$. The straight line is $(\omega+m)$.

In order to determine the physical significance of the roots shown in Fig. 5, it is necessary to examine the imaginary part of the self-energy. The spectral weight Γ of the self-energy $\Sigma(0,\omega)$, defined by

$$\Sigma(0,\omega)=\int \frac{d\omega'}{2\pi}\frac{\Gamma(\omega')}{\omega-\omega'}\ , \tag{15}$$

has the form

$$\Gamma(\omega)=\Gamma_+(\omega)\frac{1+\gamma_0}{2}-\Gamma_-(\omega)\frac{1-\gamma_0}{2}\ . \tag{16}$$

The functions $\Gamma_\pm$ are the spectral weights of $a\pm c$. From (5) we find the spectral weights to be given by

$$\Gamma_\pm=\frac{g^2}{8\pi}k_\omega\left[1\pm\frac{m}{\omega}\right]^2[(n-f)\theta(|\omega|-m) +(n+f)\theta(m-|\omega|)]\ , \tag{17}$$

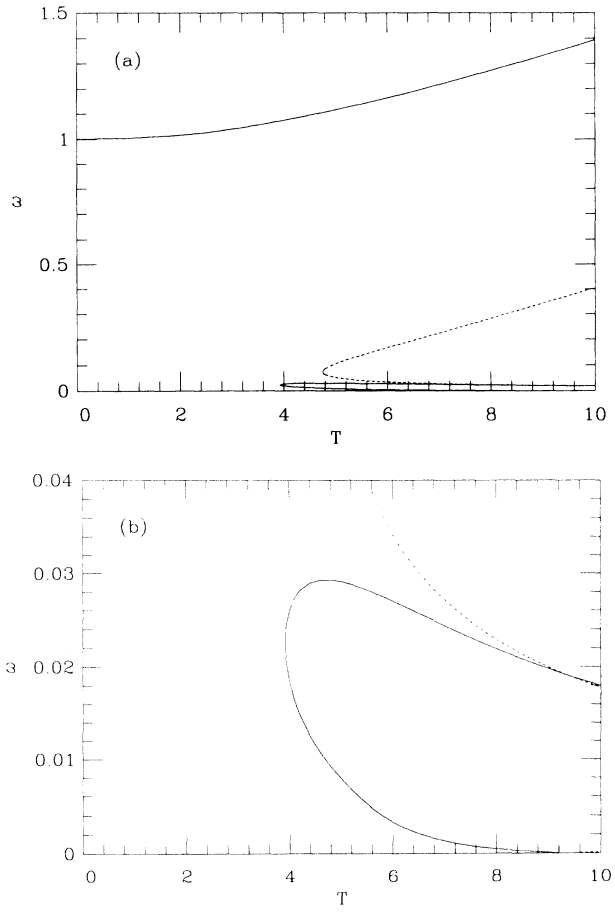

FIG. 5. (a) Positions of zeros of $\mathrm{Re}G_\pm^{-1}(\omega)$ vs temperature. Solid curves are for $\gamma_0=+1$ while dotted curves are for $\gamma_0=-1$. (b) Magnification, showing disappearance of $\gamma_0=+1$ zero and appearance of $\gamma_0=-1$ zero near $T=9$.

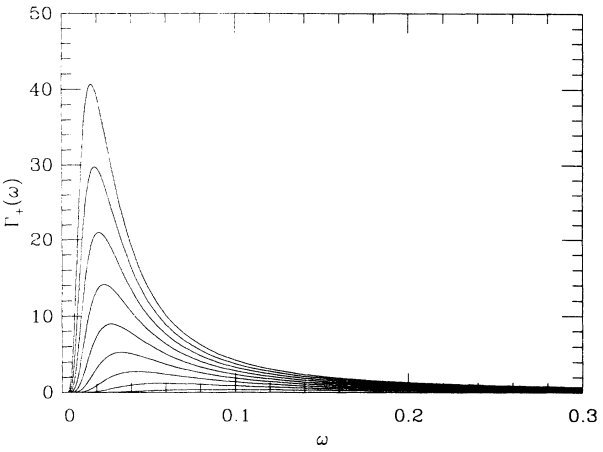

FIG. 6. Spectral weight $\Gamma_+(\omega)$ for $T=2,3\ldots,10$, in order of increasing amplitude.

where the distribution functions n and f are evaluated at $k=k_\omega=|(m^2-\omega^2)/2\omega|$. Note that $\Gamma_+/\Gamma_-=[(m+\omega)/(m-\omega)]^2$. The spectral densities $\mathcal{A}_\pm$ are then

$$\mathcal{A}_\pm(\omega)=\frac{\Gamma_\pm(\omega)}{[\omega\mp m-\mathrm{Re}(a\pm c)]^2+\Gamma_\pm^2/4}\ . \tag{18}$$

Figure 6 shows the spectral weight Γ_+ for values of T/m between 2 and 10. The characteristic feature is a sharp bunching up of $\Gamma_\pm(\omega)$ at $\omega\ll m$ for $T\gtrsim m$. (In this range of ω values, $\Gamma_+\simeq\Gamma_-$.) The reason is the following. We have already mentioned that at high temperature, the dominant processes are those in which an initial scalar photon of momentum $k\simeq T\gg m$ is absorbed, producing an electron of momentum k, or in which an initial positron of momentum k annihilates with the initial electron into a photon of momentum k. In either case, the initial electron couples to a state of low energy, $\omega\simeq m^2/k$. The increase with temperature of the number of particles in the heat bath to which the electron can couple in this way is what causes the bunching observed in Fig. 6. When $\Gamma_\pm$ is not small compared with the corresponding root of the real part of G^{-1}, as is the case for small ω/m, the root is not associated with a well-defined quasiparticle state. $\Gamma_\pm$ is clearly important for $\omega\lesssim 0.05m$.

In Fig. 7, we show the spectral densities $\mathcal{A}_\pm(\omega)$ for several values of T/m. Note that at moderate values of T/m, $\mathcal{A}_+$ has a sharp peak at $\omega\simeq m$, corresponding to the normal fermion state with $\gamma_0=+1$. In contrast, $\mathcal{A}_-$ is small for $\omega>0$. As the temperature is raised, the continuum at small ω/m in $\mathcal{A}_-$ begins to sharpen into a peak, corresponding to the upper $\gamma_0=-1$ solution displayed in Fig. 5. The peaks in $\mathcal{A}_\pm$ both survive further increase of the temperature. For temperatures between $10m$ and $50m$, the peak in $\mathcal{A}_-$ is in fact much sharper than the peak in $\mathcal{A}_+$, with the former reaching a height perhaps 100 times that of the latter at $T=20m$. At high temperature, $T\gg m$, the centroid of the two peaks is at $\omega\simeq gT/4$; their splitting is approximately m and their heights and widths are not very different.

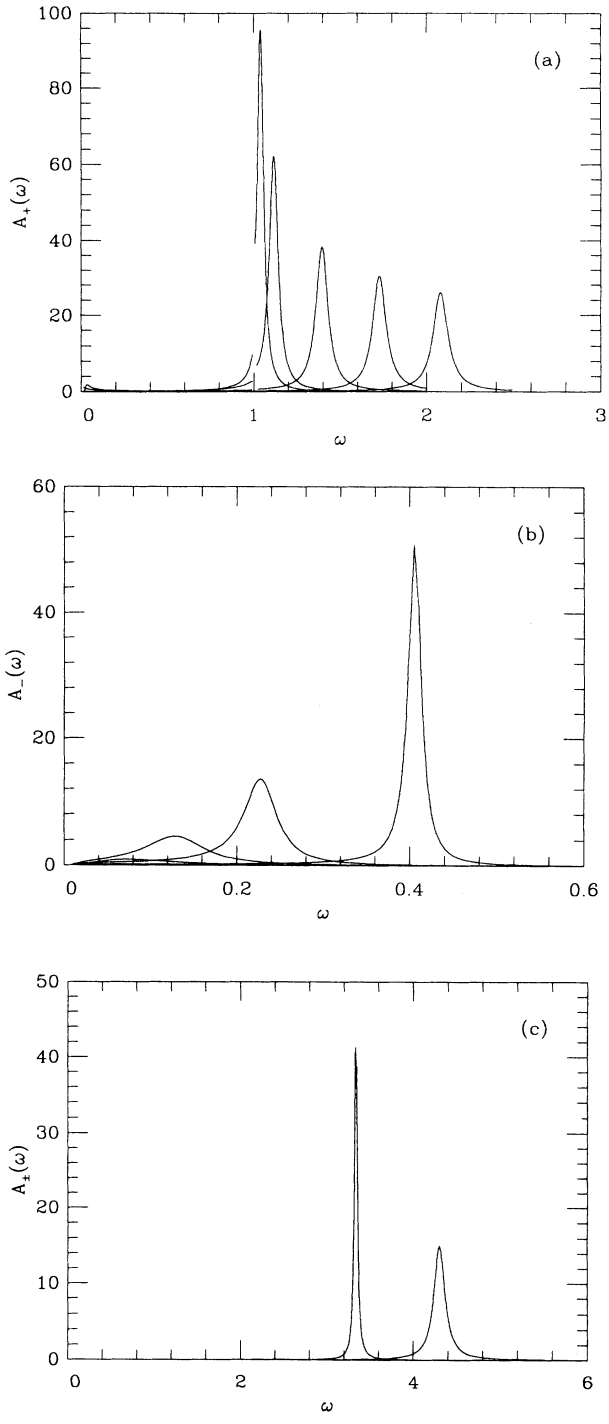

FIG. 7. (a) Spectral density $\mathcal{A}_+(\omega)$ for $T=3,5,10,15,20$ (peaks moving left to right) in Yukawa theory. The area around $\omega=1$ is omitted. (b) Spectral density $\mathcal{A}_-(\omega)$ for $T=3,5,7,10$ (peaks moving left to right). (c) Superposition of $\mathcal{A}_+(\omega)$ (right peak) and $\mathcal{A}_-(\omega)$ (left peak) for $T=50$.

III. QED

The previous section shows how the additional state in the fermion spectrum of the Yukawa theory arises through a sharpening of $\gamma_0=-1$ strength as the temperature increases. In this section we extend the discussion to the realistic case of quantum electrodynamics at finite temperature, where the results are qualitatively the same. A subtle issue is the choice of gauge. We carry out calculations in both Coulomb and Feynman gauges. In either gauge, the formulas for Σ are easily obtained from those given in Sec. II for scalar exchange. Let us first rewrite Eq. (5) in the form

$$\Sigma(0,\omega)=g^2\int\frac{d^3k}{(2\pi)^3}\int_0^\infty\frac{d\omega'}{2\pi}\rho(k,\omega')\left[\frac{\epsilon_k\gamma_0+m}{2\epsilon_k}\left[\frac{n(\omega')-f_k}{\omega-\epsilon_k-\omega'}+\frac{n(\omega')+f_k}{\omega-\epsilon_k+\omega'}\right]+\frac{\epsilon_k\gamma_0-m}{2\epsilon_k}\left[\frac{n(\omega')-f_k}{\omega+\epsilon_k+\omega'}+\frac{n(\omega')+f_k}{\omega+\epsilon_k-\omega'}\right]\right], \tag{19}$$

where

$$\rho(k,\omega)=\frac{\pi}{k}[\delta(\omega-k)-\delta(\omega+k)] \tag{20}$$

is the spectral function of the free scalar field. The photon propagator in Feynman gauge is

$$D^{\mu\nu}=\frac{g^{\mu\nu}}{k^2} \tag{21}$$

and the corresponding spectral function is simply related to ρ by

$$\rho_F^{\mu\nu}(k,\omega)=-g^{\mu\nu}\rho(k,\omega)\ . \tag{22}$$

The self-energy in Feynman gauge is then obtained by replacing $\rho(k,\omega)$ by $\rho_F^{\mu\nu}(k,\omega)$ in Eq. (19), and inserting at appropriate places the gamma matrices describing the electron-photon coupling. Using the relation

$$g^{\mu\nu}\gamma_\mu(\epsilon_k\gamma_0\pm m)\gamma_\nu=-2\epsilon_k\gamma_0\pm 4m \tag{23}$$

one easily obtains

$$a_F(\omega)=2a(\omega)\ ,\quad c_F(\omega)=-4c(\omega)\ . \tag{24}$$

In Coulomb gauge the propagator is given by

$$D^{00}(k)=\frac{1}{|\mathbf{k}|^2}\ ,\qquad D^{ij}(\omega,k)=\left[\delta^{ij}-\frac{k^ik^j}{|\mathbf{k}|^2}\right]\frac{1}{|\mathbf{k}|^2-\omega^2}\ . \tag{25}$$

It is convenient to separate the self-energy into a purely static piece $\Sigma_{\rm Coul}$ arising from the Coulomb interaction and a piece $\Sigma_{\rm trans}$ involving the interaction of the electron with the transverse photons. Proceeding as we did for Feynman gauge one easily obtains

$$a_{\rm trans}(\omega)=2a(\omega)\ ,\quad c_{\rm trans}(\omega)=-2c(\omega)\ . \tag{26}$$

In addition, the static Coulomb interaction induces a constant shift in the quasiparticle energies, given by

$$\Sigma_{\rm Coul}=-g^2\int\frac{d^3k}{(2\pi)^3}\frac{m}{\epsilon_k}\frac{1}{k^2}f_k\ . \tag{27}$$

This contribution turns out to be numerically very small.

We display in Fig. 8 the spectral densities $\mathcal{A}_\pm$ in Feyn-

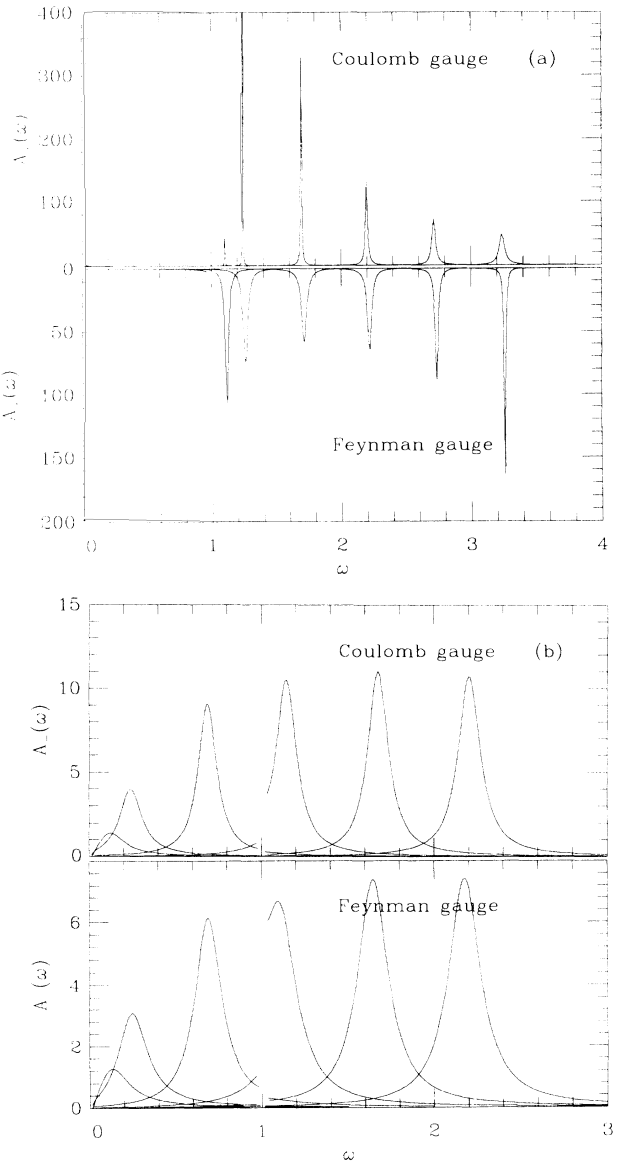

FIG. 8. (a) Spectral density $\mathcal{A}_+(\omega)$ for $T=3,5,10,15,20,25$ (peaks moving left to right) in Coulomb gauge (top) and Feynman gauge (button). The tallest peak in the Coulomb gauge plot is truncated, having a true height over 2×10^3. (b) Same for spectral density $\mathcal{A}_-(\omega)$ in both gauges.

man and Coulomb gauges. The results are similar to those for the Yukawa theory. The main quantitative result is that the new state, with $\gamma_0=-1$, rises out of the continuum at $\omega\simeq 0.1m$ when $T\simeq 3m$, when the original electron state has shifted in energy by about 10%. In terms of the coupling constant, this reads $\omega\simeq g^2m$ and $T\simeq m/g$.

A comparison of the results in the two gauges is instructive. The locations of the peaks are the same in the two gauges, while the heights of the peaks, and indeed their signs, are gauge dependent, as are their widths. The spectral densities are always positive in Coulomb gauge, where the particle content of the theory is manifest; this is not the case in Feynman gauge, where spurious states contribute. Moreover, as seen in Fig. 9, the peak in the spectral density $\mathcal{A}_+$ in the Feynman gauge changes sign when $T\simeq 29m$. This means, according to (18), that Γ_+ at the peak starts out negative at low temperatures and goes through zero at that point. Indeed, according to Eqs. (17) and (24), $\Gamma_\pm(\omega)$ in the Feynman gauge contains a factor $(1+m^2/\omega^2)\mp 4m/\omega$, so that $\Gamma_+=0$ when $\omega/m=2\pm\sqrt{3}$ at all temperatures, while Γ_- is positive for $\omega>0$ (see Fig. 10). In Coulomb gauge, on the other hand, $\Gamma_\pm(\omega)\propto(1\mp m/\omega)^2\geq 0$.

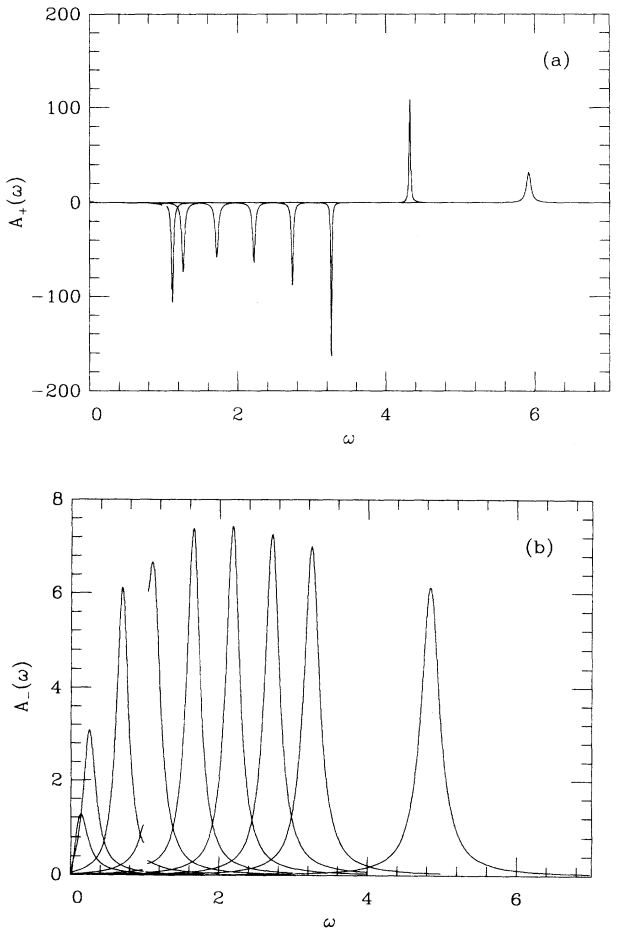

FIG. 9. (a) Feynman gauge spectral density $\mathcal{A}_+(\omega)$ for $T=3,5,10,15,20,25,35,50$ (peaks moving left to right). (b) Spectral density $\mathcal{A}_-(\omega)$ for $T=3,5,10,15,20,25,30,35,50$ (peaks moving left to right). Note change in scale relative to (a).

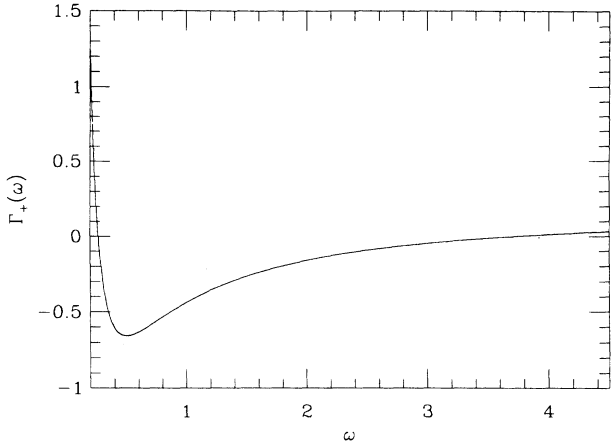

FIG. 10. Feynman gauge spectral weight $\Gamma_+(\omega)$ for $T=30$. The region $\omega<0.2$ is suppressed. The function rises to a peak value $\Gamma_+\simeq 2075$ at $\omega\simeq 0.0055$. As the temperature is raised, the amplitude of the spectral weight increases as in Fig. 6, with the zeros remaining at $\omega=2\pm\sqrt{3}$.

This gauge dependence of the spectral function is very much reminiscent of the problems encountered in the calculation of the gluon damping rate, and points to the inconsistency for the one-loop calculation of the spectral function. In particular, while the energies of the quasiparticles are of order gT, their widths are of order g^2T. Contributions of order gT are entirely contained in the one-loop calculation. This is not the case for the terms of order g^2T which receive contributions from multiloop processes. A fully consistent calculation of the spectral functions should incorporate these higher-order effects, and indeed once this is done, a gauge-invariant and positive value is obtained for the width of the quasiparticles [6,12].

However, this discussion should not be allowed to obscure the physics correctly identified in the one-loop calculation. As we have seen, the new quasiparticle emerges gradually in the system as the temperature is raised, from accumulation of single particle strength at small energy. This accumulation is due to processes similar to those responsible for Landau damping in an ordinary plasma, and gives the new mode a collective character. The resulting peak in $\Gamma(\omega)$ grows with the temperature and its existence is obviously independent of the choice of gauge. [Note in particular in Fig. 10 that the absolute value of $\Gamma_+(\omega)$ in the region where it is negative is very much smaller than the height of the peak at small ω.] Via the usual dispersion relation, the peak at small ω in the imaginary part of the self-energy induces the $1/\omega$ behavior of the real part which is ultimately the cause for the existence of two quasiparticle peaks in the electron propagator. The new quasiparticle emerges at an energy located away from the peak in Γ, the more so the higher the temperature. Therefore, the new quasiparticle very quickly finds itself in a region where Γ is small, and its energy is then entirely determined by the real part of Σ,

correctly given by the one-loop calculation. Indeed the real part of Σ in the one-loop approximation depends very weakly on the gauge in which it is calculated; the pole positions are independent of the gauge.

IV. THE ZERO-TEMPERATURE PROPAGATOR

In Secs. II and III we considered only the finite-temperature part of the self-energy Σ. In point of fact, $\Sigma=\Sigma_0+\Sigma_T$, where Σ_T vanishes at $T=0$ and Σ_0 is the zero-temperature part of the self-energy. We have so far taken only Σ_T into account. Now we study the influence of the zero-temperature piece Σ_0 on the quasiparticle properties. Since the deviation of the original electron state from the mass shell is of order gT, these terms are potentially important when $gT \gg m$. They could also be important for the new $\gamma_0=-1$ quasiparticle right from its appearance, since it appears well off the electron mass shell.

At zero temperature, the electron propagator can be written

$$G^{-1}(\mathbf{p}=0,\omega)=(\omega-a_0)\gamma_0-(c_0+m)\ , \tag{28}$$

so that

$$\Sigma_0(0,\omega)=a_0\gamma_0+c_0\ . \tag{29}$$

Both a_0 and c_0 are divergent. Following a standard procedure, we absorb the divergences into renormalization constants which are a correction to the mass δm and a field renormalization Z_2. The finite parts of these counterterms are fixed by demanding that in the vicinity of $\omega=m$ the propagator behaves as that of a free particle with mass m. The renormalization constants appear in the renormalized propagator as

$$G_R^{-1}(\mathbf{p}=0,\omega)=Z_2[(\omega-a_0)\gamma_0-(c_0+m)+\delta m]\ . \tag{30}$$

The renormalization conditions give

$$\begin{aligned} Z_2^{-1}-1&=-\left.\frac{\partial a_0}{\partial\omega}\right|_m-\left.\frac{\partial c_0}{\partial\omega}\right|_m\ ,\\ \delta m&=a_0(m)+c_0(m)\ . \end{aligned} \tag{31}$$

The renormalized propagator then takes the form

$$\begin{aligned} G_R^{-1}(\mathbf{p}=0,\omega)=\omega\gamma_0&\left[1-\frac{a_0(\omega)}{\omega}+\left.\frac{\partial(a_0+c_0)}{\partial\omega}\right|_m\right]\\ &-m\left[1-\left.\frac{\partial(a_0+c_0)}{\partial\omega}\right|_m\right.\\ &\left.+\frac{c_0(\omega)-c_0(m)-a_0(m)}{m}\right]\ . \end{aligned} \tag{32}$$

G_R as given in (32) is ultraviolet finite. As is well known, however, the integrals contributing to Z_2, i.e., the integrals giving the derivatives of the self-energy with respect to ω at $\omega=m$, are also infrared divergent and so is G_R. They can be regularized by assigning a small mass λ to the photon. Once this is done, the renormalized propagator may be written in the form

$$G_R^{-1}(\omega)=[\omega-a_R(\omega)]\gamma_0-m-c_R(\omega)\ , \tag{33}$$

where $a_R(\omega)$ and $c_R(\omega)$ are finite functions of ω which depend on the infrared cutoff λ. For the scalar case, one has

$$\begin{aligned} \frac{a_R(\omega)}{\omega}&=\frac{\alpha}{4\pi}(K_a-L_a-L_c)\ ,\\ \frac{c_R(\omega)}{m}&=\frac{\alpha}{4\pi}(K_c+L_a+L_c)\ , \end{aligned} \tag{34}$$

where K_a, K_c, L_a, and L_c are integrals to be given below. The corresponding formulas for QED are easily obtained from Eqs. (34) by multiplying the integrals $K_{a,c}$ and $L_{a,c}$ by simple numerical factors. For Feynman gauge, K_a and L_a are multiplied by 2, while K_c and L_c are multiplied by -4. For Coulomb gauge, K_a and L_a are multiplied by 2, while K_c and L_c are multiplied by -2.

The integrals $K_{a,c}$ and $L_{a,c}$ depend on the infrared cutoff λ. However, in the limit $\lambda\to 0$, K_a and K_c are finite and are given by

$$\begin{aligned} K_a(\omega)&=\tfrac{1}{2}\left[1-\frac{m^2}{\omega^2}\right]+\tfrac{1}{2}\left[1-\frac{m^4}{\omega^4}\right]\ln\left[1-\frac{\omega^2}{m^2}\right]\ ,\\ K_c(\omega)&=\left[1-\frac{m^2}{\omega^2}\right]\ln\left[1-\frac{\omega^2}{m^2}\right]\ . \end{aligned} \tag{35}$$

When $\omega \gg m$,

$$\begin{aligned} K_a(\omega)&\sim\tfrac{1}{2}\ln\left[\frac{\omega^2}{m^2}\right]-i\pi\ ,\\ K_c(\omega)&\sim\ln\left[\frac{\omega^2}{m^2}\right]-i\pi\ . \end{aligned} \tag{36}$$

The infrared divergent integrals L_a and L_c are independent of ω and given explicitly by

$$\begin{aligned} L_a&=-2\int_0^1 dx\frac{x^2(1-x)}{(1-x)^2+x\lambda^2/m^2}\ ,\\ L_c&=-2\int_0^1 dx\frac{x(1-x)}{(1-x)^2+x\lambda^2/m^2}\ . \end{aligned} \tag{37}$$

In the limit $\lambda\to 0$ these integrals behave as

$$\begin{aligned} L_a&=3+\ln\frac{\lambda^2}{m^2}+\mathcal{O}\left[\frac{\lambda}{m}\right]\ ,\\ L_c&=2+\ln\frac{\lambda^2}{m^2}+\mathcal{O}\left[\frac{\lambda}{m}\right]\ . \end{aligned} \tag{38}$$

Let us now analyze the influence of $a_R(\omega)$ and $c_R(\omega)$ on the quasiparticle masses. We restrict ourselves to the scalar case. It is not difficult to show that the $T=0$ terms do not have much effect at small temperatures, $T\simeq 3m$, when the new quasiparticle emerges. Indeed, at small ω, K_a and K_c are well behaved [$K_a(x)\sim 1-x^2/2$ and $K_c(x)\sim 3/4-x^2/3$ where $x=\omega/m$], and the dominant effect of the $T=0$ terms, $a_R\pm c_R$, is to shift $c(0)$ to $c(0)+(\alpha m/2\pi)\ln(\lambda^2/m^2)$, where λ is the photon mass. Since $c(0)\approx-\alpha\pi T^2/2m$ [see Eq. (13)], the effect of the

new term is negligible unless $\lambda^2/m^2 \sim \exp(-\pi^2 T^2/m^2)$, which is already a very small value when $T \sim m$. Similarly, when $\omega, T \gg m$, i.e., in the vicinity of the quasiparticle energies at high temperature, the equation for the poles, $\omega - m - \mathrm{Re}(a + a_R = c + c_R) = 0$, becomes

$$\omega^2 \left[1 - \frac{\alpha}{4\pi} \left[\ln\frac{\omega}{m} - \ln\frac{\lambda^4}{m^4} \right] \right] = \frac{\alpha\pi}{4} T^2 , \tag{39}$$

where we have neglected the terms of order $m \ll T$, and kept only the logarithmic term in L_a. The function on the left-hand side of this equation has a maximum at $\omega/m \approx (\lambda/m)^4 \exp(4\pi/\alpha)$. If the temperature is so high that the value of the function at this maximum equals $\alpha\pi T^2/4$, our calculation ceases to make sense. But unless the cutoff λ is very small this possibility occurs only for extremely high temperature, of order $m(\lambda/m)^4 \exp(4\pi/\alpha)$. Therefore, unless the cutoff λ takes an exceedingly small value (on the scale of m or T), one can safely ignore the $T=0$ counterterms. However, as a question of principle, the presence of this infrared cutoff indicates that one must be more careful in defining quasiparticle states at finite temperature when they involve coupling to massless particles. This issue deserves further investigation.

V. CONCLUSIONS

We have discussed how in a QED plasma at high temperature a new quasiparticle, the plasmino, can appear alongside the ordinary electron state. We have shown that this new quasiparticle gradually emerges in the system as the temperature rises. The mechanism responsible for the apparition of this new state is a buildup of single particle strength at small ω caused by the coupling between the electron and an increasing number of low-energy particles, through processes reminiscent of Landau damping in ordinary plasmas.

Our analysis is based on a one-loop calculation, and as such is subject to criticism. It is now well known that, while the one-loop calculation gives the dominant contribution to the dispersion relation at high temperature, this is not so for the full spectral function, as is apparent in our illustrative comparison between Coulomb and Feynman gauge spectral functions. It is not clear whether higher-loop corrections would change our results materially, especially in the temperature range in which the new quasiparticle emerges. We believe however that our main conclusion that the structure in the spectrum develops gradually rather than in a discrete transition would survive such corrections, as this is mostly determined by well-identified physical processes.

Finally, our study of the role of the zero-temperature counterterms point to another difficulty. We have seen that these counterterms are infrared divergent and, when regularized, depend on a cutoff λ. In calculations of physical processes at zero temperature, the cutoff dependence originating from various contributions cancels out. We can expect a similar cancellation to take place at finite temperature; however, the very definition of a quasiparticle requires refinement.

ACKNOWLEDGMENTS

We are grateful for the hospitality of the Physics and Theoretical Divisions of Los Alamos National Laboratory, where we began the collaboration reported here. We thank J. Y. Ollitrault, I. Paziashvili, A. Smilga, and A. Weldon for helpful conversations. This work was supported in part by National Science Foundation Grants Nos. DMR88-18713 and DMR91-22385. The work of B.S. was supported in part by a Wolfson Research Award administered by the Israel Academy of Sciences and Humanities, by the German-Israel Foundation, and by the Center for Absorption in Science of the Israel Ministry of Immigrant Absorption.

[1] V. Klimov, Yad. Fiz. **33**, 1734 (1981) [Sov. J. Nucl. Phys. **33**, 934 (1981)].
[2] V. Klimov, Zh. Eksp. Teor. Fiz. **82**, 336 (1982) [Sov. Phys. JETP **55**, 199 (1982)].
[3] H. A. Weldon, Phys. Rev. D **26**, 2789 (1982).
[4] H. A. Weldon, Phys. Rev. D **40**, 2410 (1989).
[5] V. V. Lebedev and A. V. Smilga, Ann. Phys. (N.Y.) **202**, 229 (1990).
[6] R. D. Pisarski, in *Quark Matter '88,* Proceedings of the 7th International Conference on Ultrarelativistic Nucleus-Nucleus Collisions, Lenox, Massachusetts, edited by G. Baym, P. Braun-Munzinger, and S. Nagamiya [Nucl. Phys. **A498**, 423c (1989)].
[7] E. Petitgirard, Report No. LAPP-TH-346/91, 1991 (unpublished).
[8] E. Braaten and R. Pisarski, Phys. Rev. Lett. **64**, 1338 (1990); Nucl. Phys. **B337**, 569 (1990); Phys. Rev. D **42**, 2156 (1990); Nucl Phys. **B339**, 310 (1990).
[9] J. P. Blaizot and J. Y. Ollitrault (in preparation).
[10] R. Kobes, G. Kunstatter, and A. Rebhan, Phys. Rev. Lett. **64**, 2992 (1990).
[11] R. Kobes, G. Kunstatter, and A. Rebhan, Nucl. Phys. **B355**, 1 (1991).
[12] E. Braaten and R. Pisarski, Phys. Rev. D **46**, 1829 (1992).
[13] H. A. Weldon, Physica **A158**, 169 (1989).